TISSUE ENGINEERING: Part A
Volume 20, Numbers 3 and 4, 2014

DOI: 10.1089/ten.tea.2013.0222

Enhancement of BMP-2 Induced Bone Regeneration by SDF-1α Mediated Stem Cell Recruitment

Stefan Zwingenberger, MD,[1,2] Zhenyu Yao, MD, PhD,[1] Angela Jacobi, PhD,[2] Corina Vater, PhD,[2] Roberto D. Valladares,[1] Chenguang Li,[1] Christophe Nich, MD, PhD,[1,3,4] Allison J. Rao,[1] Jane E. Christman,[1] Joseph K. Antonios,[1] Emmanuel Gibon, MD,[5] Axel Schambach, MD, PhD,[6] Tobias Maetzig, PhD,[6] Stuart B. Goodman, MD, PhD,[1] and Maik Stiehler, MD, PhD[2]

Treatment of critical size bone defects is challenging. Recent studies showed that the cytokine stromal cell-derived factor 1 alpha (SDF-1α) has potential to improve the bone regenerative effect of low bone morphogenetic protein 2 (BMP-2) concentrations. The goal of this study was to demonstrate the combined effect of SDF-1α and BMP-2 on bone regeneration and stem cell recruitment using a critical size femoral bone defect model. A total of 72 mice were randomized to six groups. External fixators were implanted onto the right femur of each mouse and 3 mm defects were created. Depending on the group affiliation, adenovirally activated fat tissue grafts expressing SDF-1α or/and BMP-2 were implanted at the defect site. One day after operation, 1×10^6 murine mesenchymal stromal cells (MSCs), lentivirally transduced to express the gene enhanced green fluorescent protein (eGFP), firefly luciferase, and CXCR4 were injected systemically in selected groups. Migration of the injected MSCs was observed by bioluminescence imaging on days 0, 2, 4, 6, 8, 10, 12, 14, 21, 28, and 42. After 6 weeks, animals were euthanized and 80 μm CT-scans were performed. For histological investigations, hematoxylin and eosin-, tartrate-resistant acid phosphatase-, alkaline phosphatase-, and anti-eGFP-stained sections were prepared. BMP-2 and SDF-1α combined at the defect site increased bone volume (BV) (2.72 mm^3; 95% CI 1.95–3.49 mm^3) compared with the negative control group (1.80 mm^3; 95% CI 1.56–2.04 mm^3; $p < 0.05$). In addition, histological analysis confirmed a higher degree of bone healing in the BMP-2 and SDF-1α combined group compared with the negative control group. Bioluminescence imaging demonstrated higher numbers of migrated MSCs toward the defect site in the presence of both BMP-2 and SDF-1α at the defect site. Furthermore, eGFP-labeled migrated MSCs were found in all defect areas, when cells were injected. The ratio of osteoblasts to osteoclasts, assessed by immunohistological staining, was higher and thus showed a trend toward more bone formation for the combined use of BMP-2 and SDF-1α compared with all other groups. This study demonstrated that SDF-1α enhanced BMP-2 mediated bone healing in a critical size segmental bone defect model. Notably, both proteins alone also provided a cumulative effect on MSC attraction toward the site of injury.

Introduction

Localized bone loss associated with trauma, tumor, infection, periprosthetic osteolysis, or congenital musculoskeletal disorders denotes a major worldwide socioeconomic problem frequently requiring surgical intervention. According to data from the U.S. Health Cost and Utilization Project, there were ~1 million hospital admissions for appendicular skeletal fractures in the USA, with aggregate costs of over $26 billion.[1] Approximately 10% of all fractures are complicated with impaired healing.[2] Furthermore, the number of patients suffering from aseptic implant loosening frequently associated with extensive periprosthetic bone loss, pain, and loss of function is constantly increasing. Autologous bone grafting is the gold standard for the treatment of extensive osseous defects, however, the procedure is associated with

[1]Department of Orthopaedic Surgery, Stanford University, Stanford, California.
[2]Department of Orthopaedics, University Hospital Carl Gustav Carus at Technische Universität Dresden, Dresden, Germany.
[3]Laboratoire de Biomécanique et Biomatériaux Ostéo-Articulaires—UMR CNRS 7052, Faculté de Médecine, Université Paris 7, Paris, France.
[4]Department of Orthopaedic Surgery, European Teaching Hospital, Assistance Publique—Hôpitaux de Paris, Université Paris 5, Paris, France.
[5]Department of Orthopaedic Surgery, Bichat Teaching Hospital, Paris School of Medicine, Paris, France.
[6]Institute of Experimental Hematology, Hannover Medical School, Hannover, Germany.

potential donor-site morbidity, for example, neurovascular injury, fracture, infection, prolonged pain, and cosmetic issues.[3,4] In addition, the quantity of autologous bone is limited in a given individual.

The growth factor bone morphogenetic protein 2 (BMP-2) is FDA approved since 2002 and has been clinically established for lumbar spine fusion and repair of open tibia fractures.[5] van Baardewijk *et al.* reported median systemic BMP-2 levels of 641 pg/mL in patients with physiological fracture healing 4.9 years (range 2.01–8.56) after bone healing.[6] The concentration approved for clinical use is 1500 μg/mL, and thus 2×10^6-fold higher.[6] Zara *et al.* investigated various concentrations of BMP-2 in a critical size femoral rat defect model.[7] Low concentrations of 5 to 10 μg/mL BMP-2 did not induce defect fusion, midrange BMP-2 concentrations of 30 μg/mL led to fusion of the defect without adverse effects, and high BMP-2 concentrations of 150 to 600 μg/mL resulted in additional cyst-like bony shells filled with adipose tissue and induced tissue inflammatory infiltrates and exudates. Within the last few years, there has been an increasing number of clinical reports concerning the severe side effects of BMP-2 used at high local doses, for example, ectopic bone formation associated with an increased incidence of paralysis due to spinal cord or nerve damage.[8–10] Furthermore, bowel-, bladder- and sexual-dysfunctions as well as a greater apparent risk of new malignancy were reported in association with usage of higher doses of rhBMP-2.[8–10]

Mesenchymal stromal cells (MSCs) are progenitor cells present in several adult tissues that are capable of differentiating into bone cells. They are involved in the initiation of the fracture repair process leading to the formation of a cartilaginous template (callus) preceding local bone regeneration.[11] Consequently, MSCs have a high therapeutic potential in patients with fractures to reduce the time of healing and to treat nonunions.

The cytokine stromal cell-derived factor 1 alpha (SDF-1α) has been shown to attract MSCs using the CXCR4 cell-surface receptor both *in vitro* and *in vivo*.[12] Recently, it has been reported that the combination of low dose BMP-2 and SDF-1α results in an increased rate of bone healing.[13] However, this has not been tested in a critical size femoral bone defect yet.

The aim of this study was to investigate the combined effects of BMP-2 and SDF-1α on bone formation and systemic recruitment of MSCs applying a recently validated[14] murine femoral critical size bone defect model.

Materials and Methods

Animals and experimental design

A total of 72 12-week-old nu/nu nude mice (Charles River Laboratory, Inc., Wilmington, MA) were housed and fed at the Research Animal Facility at Stanford University. The experimental design was approved by the local Institutional Administration Panel for Laboratory Animal Care (protocol number 26905). Mice were randomized into six groups ($n=12$ each, Table 1). One surgeon implanted external fixators onto the right femur of each mouse and created a 3 mm midshaft femoral defect. Depending on the group affiliation, adenoviral activated fat tissue grafts expressing SDF-1α or/and BMP-2 or red fluorescent protein (RFP) were implanted at the defect site. For the negative control group, the defect site was kept empty. One day after the operation, also group related, 1×10^6 genetically altered reporter MSCs expressing the genes for enhanced green fluorescent protein (eGFP), firefly luciferase, and human CXCR4 (CXCR4) were administered by intracardiac injection. The negative control group received no MSC injection. Migration of the injected MSCs was explored by bioluminescence imaging on days 0, 2, 4, 6, 8, 10, 12, 14, 21, 28, and 42. The postoperative observation period was 6 weeks. After 6 weeks, animals were euthanized by cervical dislocation following anesthesia. A microcomputed

Table 1. Description of the Experimental Groups

Group	*1 BMP-2, SDF-1α, CXCR4(+) MSCs*	*2 BMP-2, CXCR4(+) MSCs*	*3 SDF-1α, CXCR4(+) MSCs*	*4 SDF-1α, CXCR4(−) MSCs*	*5 Control fat tissue, CXCR4(−) MSCs*	*6 No fat tissue, no MSCs*
SDF-1α expressing fat tissue graft	X		X	X		
BMP-2 expressing fat tissue graft	X	X				
Control (only RFP expressing fat tissue graft)					X	
No fat tissue graft						X
Intracardiac injection of CXCR4(+) MSCs	X	X	X			
Intracardiac injection of CXCR4(−) MSCs (control)				X	X	
No MSC injection						X
Number of animals available for complete evaluation (original number of animals in the group)	10 (12)	8 (12)	11 (12)	8 (12)	10 (12)	11 (12)

For the treatment groups (groups 1–5), adenovirally activated fat tissue grafts expressing human stromal cell-derived factor 1 alpha (SDF-1α), human bone morphogenetic protein 2 (BMP-2), or only red fluorescence protein (RFP) were inserted at the defect site. Mice received lentivirally transduced mesenchymal stromal cells (MSCs) expressing the marker genes for enhanced green fluorescent protein (eGFP) and firefly luciferace through intracardiac injection. These MSCs were group-related overexpressing human CXCR4 receptor [CXCR4(+)] or were negative for human CXCR4 receptor [CXCR4(−)]. The negative control group (group 6) received no fat tissue graft as well as no intracardiac MSC injection. One to four animals per group were lost during the observation period due to tumor growth, pulmonary embolism, or bleeding after intracardiac injection.

tomography (μCT) scan was done on each femur. For histological investigations, hematoxylin and eosin (H&E), tartrate-resistant acid phosphatase (TRAP), alkaline phosphatase, and anti-eGFP stains were prepared.

Isolation and lentiviral transduction of the MSCs

Primary murine MSCs were harvested, expanded up to passage 4, and characterized according to the protocol of Zhu *et al.*[15] The cumulative numbers of population doublings in passage 4 were 14–18, including initial colony formation. Cells were transduced by lentiviral vectors encoding the genes for eGFP, firefly-luciferase, and CXCR4. Efficient transduction and expression of the genes for a minimum period of 6 weeks was proven by fluorescence activated cell sorting, fluorescence imaging, and bioluminescence imaging as described previously.[16]

Harvesting and adenoviral transduction of fat tissue grafts

Primary murine fat tissue was harvested from the anterolateral proximal hind legs of five eight-week-old C57/BL6 mice (Jackson, Bar Harbor, ME). Spherical tissue grafts with a diameter of 3 mm were transduced by 10 μL of adenoviral vector (2×10^8 plaque forming units per sample; Vector BioLabs, Philadelphia, PA) containing solution to express transgenes encoding for human BMP-2, human SDF-1α, or RFP (sham group). The transduction was performed according to the protocol of Betz *et al.*[17] Successful transduction and long-term expression were assessed by analyzing cell culture supernatants using ELISA (Quantikine, hSDF-1α and BMP-2 Immunoassay; R&D Systems GmbH, Wiesbaden, Germany).

Surgery and systemic MSC administration

The implantation of the external fixator and creation of the 3 mm bone defect were performed as described recently.[14] The adenoviral activated fat tissue grafts were implanted within the defect and the wound was closed by interrupted sutures. On the first postoperative day, mice were placed under anesthesia in the supine position and reporter cells were administered by left ventricular intracardiac injection. Successful injection was proven immediately postinjection by bioluminescence imaging.

Bioluminescence imaging

In vivo bioluminescence imaging was performed using the IVIS Spectrum system (Caliper Life Science, Hopkinton, MA). Animals were anesthetized with 2% isoflurane during the process. Each mouse received 6 mg D-Luciferin (Biosynth AG, Staad, Switzerland) in 0.2 mL phosphate-buffered saline (Thermo Fisher Scientific, Waltham, MA) by intraperitoneal injection. Ten minutes after injection, whole-body images of each mouse were taken. Standardized regions of interest (ROI) (1.2×0.5 cm; Fig. 2) at the level of the diaphyseal femur were investigated bilaterally. Bioluminescence was expressed as photon/second/cm^2/steradian.

Radiographs and μCT

Anesthesia was maintained by mask inhalation of isoflurane and animals were placed in the ventral position in the MicroCAT II μCT scanner (ImTek, Inc., Knoxville, TN). During the postoperative observation time, this device was used to stabilize the body to take radiographs.

For μCT, after 6 weeks, all femurs were scanned using the MicroCAT II μCT scanner. Before imaging, scout radiographs were taken to ensure that the femurs were entirely scanned. The following settings were used: x-ray tube potential (peak) was 80 kVp, x-ray intensity was 0.25 mAs, with an integration time of 0.5 s, for each of the 360 rotational steps. The projection data were reconstructed into tomograms following a Feldkamp algorithm using a commercial software package (Cobra EXXIM; EXXIM Computing Corp., Livermore, CA) at 80 μm isotropic voxel size. Every scan was conducted with a phantom containing samples of hydroxyapatite, water, and air. This was used to calibrate all scans to produce isosurfaces standardized at 700 Hounsfield units to allow for accurate comparisons between scans. Using the imaging software Microview (GE Medical Systems, Fairfield, CT), a standardized three-dimensional ROI (Fig. 3) was created (3.5×2.5×2.5 mm) for BV and bone mineral density (BMD) assessment. The ROI was aligned centrally between the inner two pins of the external fixator. BV and BMD data were presented as mm^3 and mg/cc, respectively.

Histology

Femora were decalcified using paraformaldehyde (PFA) for 3 days followed by ethylenediaminetetraacetic acid (EDTA) twice for 7 days each. Longitudinal frozen sections of 5 μm were cut using a cryostat (Cambridge Instruments, Buffalo, NY). All slides were fixed in acetone.

To evaluate the histomorphology of bone healing, slides were stained for H&E (Sigma-Aldrich, Steinheim, Germany). Three representative sections per femur were analyzed by light microscopy (50× magnification, Olympus BX 50; Olympus Optical Co., Tokio, Japan) and software package (SPOT Imaging Solutions, Sterling Heights, MI). Histological grading of fracture healing was classified according to Huo *et al.*[18]

To evaluate bone metabolism, the ratio of osteoblasts to osteoclasts in the former defect area was quantified. Osteoclast-like cells were identified as multinuclear cells using a leukocyte acid phosphatase kit (TRAP staining; Sigma-Aldrich, Co., St. Louis, MO). Cells with an osteoblastic phenotype were identified by an alkaline phosphatase staining (Vector Laboratories, Inc., Burlingame, CA). TRAP-positive and alkaline phosphatase-positive cells in the former defect area were counted (200× magnification; Olympus BX 50).

To identify the systemically administered, migrated reporter MSCs in the defect area, anti-GFP immunofluorescence staining (BD, Franklin Lakes, NJ) was performed. Standardized images were taken (50× magnification, Observer.Z1; Carl Zeiss, Jena, Germany) and numbers of green pixels per area were determined using ImageJ v1.44p software (U. S. National Institutes of Health, Bethesda, MD).

Statistics

For sample size calculation, it was anticipated that data obtained from rat studies can be transferred to mouse experiments using a scale factor. Because the investigation presented here had not been performed before calculation of the needed number of animals, the number was based on a

previous study that investigated the therapy of critical size (5 mm) femur defects in rats by BMP-2 activated muscle tissue.[17] To reach a statistical power of 80% at a significance level of $\alpha = 5\%$ by simple linear contrasts between the different groups, a group size of $n = 10$ was needed. To compensate for possible drop-outs due to death of animals as a consequence of infection, blood loss, etc., two additional animals were added per group resulting in a total of $N = 72$ animals for all six groups.

Numerical data were statistically analyzed using Graphpad Prism 5.00 software (San Diego, CA). The results are presented as mean and 95% confidence interval (95% CI). Since data followed a Gaussian distribution, statistical significance was tested by one-way ANOVA. For *post hoc* testing, the individual treatment groups were tested applying the Tukey's multiple comparison test versus the negative control group. The level of significance was set at $p = 0.05$. Analysis of bioluminescence imaging, BV, immunohistological staining for migrated MSCs, osteoclast and osteoblast counts were performed quantitatively, and histomorphology was analyzed semiquantitatively.

Results

Evaluation of transgene expression by the adenovirally transduced fat tissue grafts *in vitro* is summarized in Figure 1. Using the adenoviral vector Ad-SDF-BMP, expression levels of both SDF-1α and BMP-2 comparable to those of SDF-1α (Ad-SDF-RFP) and BMP-2 (Ad-RFP-BMP) alone, respectively, were observed. SDF-1α and BMP-2 transgene expression was detectable up to 2 and 3 weeks, respectively.

All of the animals survived the operations. Fifty-eight out of 72 animals reached the sixth postoperative week (Table 1). One to four animals per group died before the end of the observation period due to tumor growth ($n = 1$), pulmonary embolism ($n = 6$), or bleeding following intracardiac injection ($n = 7$).

Migration of the systemically administered MSCs to the critical size segmental femoral defect was assessed *in vivo* by bioluminescence imaging (Fig. 2). The strongest bioluminescent signal in the region of interest (segmental bone defect, right femur) was detected in the BMP-2, SDF-1α, CXCR4(+) reporter MSC group. Similarly, this group showed the highest intraindividual difference of the bioluminescent signal between the right and the left femur.

The BV after the observation time of 6 weeks was evaluated by μCT (Fig. 3). The highest BV in the region of interest (former defect area) was found in the BMP-2, SDF-1α, CXCR4(+) MSC group. The negative control group showed a tendency to more bone regenerate than all treatment groups having only BMP-2 or only SDF-1α at the defect site.

To evaluate the degree of bone healing histologically, we applied a scoring system described by Huo *et al.*[18] (Fig. 4). The BMP-2, SDF-1α, CXCR4(+) MSC group showed the highest degree of bone healing with a mean score of 5.3 (95% CI 4.6–6.0) corresponding to predominantly cartilaginous tissue in the former defect with an equal ratio of bone to fibrous tissue. The other groups were scored between 1.6 (95% CI 1.4–1.8) and 3.0 (95% CI 2.7–3.3) denoting significant less bone formation ($p < 0.05$) with mainly fibrous tissue and small amounts of cartilage. The negative control group was scored 3.0 (95% CI 2.7–3.3) being significantly higher compared with the groups, SDF-1α, CXCR4(+) MSCs (1.8 [95% CI 1.6–2.0]); SDF-1α, CXCR4(−) MSCs (1.6 [95% CI 1.4–1.8]); and control fat tissue, CXCR4(−) MSCs (1.7 [95% CI 1.5–1.9]) (each $p < 0.05$).

Using immunohistological staining, systemically administered eGFP-labeled MSCs were detected in the defect areas. EGFP-positive MSCs were mainly found within the fibrous and remaining fat tissue in the central area of the defect. To a lesser degree, however, they were also detected within woven bone (Fig. 5). Only a few of these MSCs were found within the bone marrow. Comparing the number of green pixels, denoting the presence of labeled MSCs, significantly higher numbers of migrated MSCs were found in the BMP-2, SDF-1α, CXCR4(+) MSC group than in all other groups ($p < 0.05$, Tukey test). In the case of expression of BMP-2 or SDF-1α alone at the defect side, about the same number of labeled MSCs was attracted. As no positive green pixels were found in the absence of MSCs, the autofluorescence intensity of the tissue was below detection range of the fluorescence microscopy analysis.

Using immunohistological staining, the ratio of osteoblasts to osteoclasts in the former defect area was analyzed to

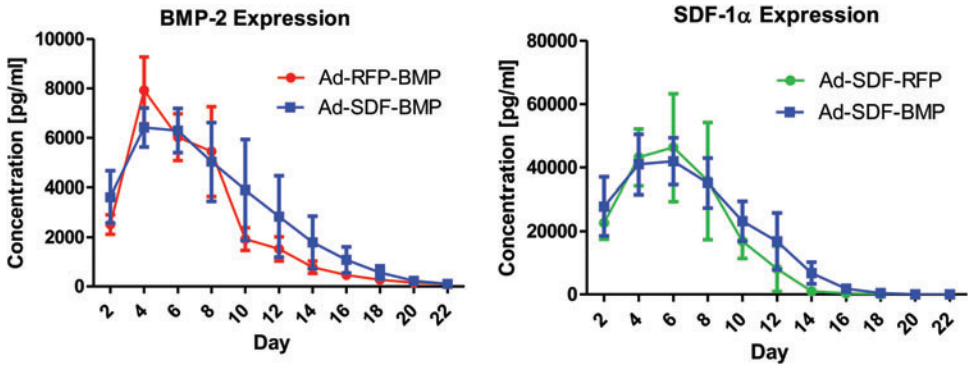

FIG. 1. *In vitro* transgene expression levels by adenovirally (Ad-SDF-BMP, Ad-SDF-RFP, and Ad-RFP-BMP) transduced fat tissue grafts were assessed *in vitro* up to 22 days using SDF-1α and BMP-2 ELISA ($n = 3$ for each time point). Ad-SDF-BMP transduction resulted in temporal expression levels of both SDF-1α and BMP-2 comparable to transduction by the single-target gene vectors Ad-SDF-RFP and Ad-RFP-BMP. Bone morphogenetic protein 2 (BMP-2), stromal cell-derived factor 1 alpha (SDF-1α), red fluorescent protein (RFP), enzyme-linked immunosorbent assay (ELISA). Color images available online at www.liebertpub.com/tea

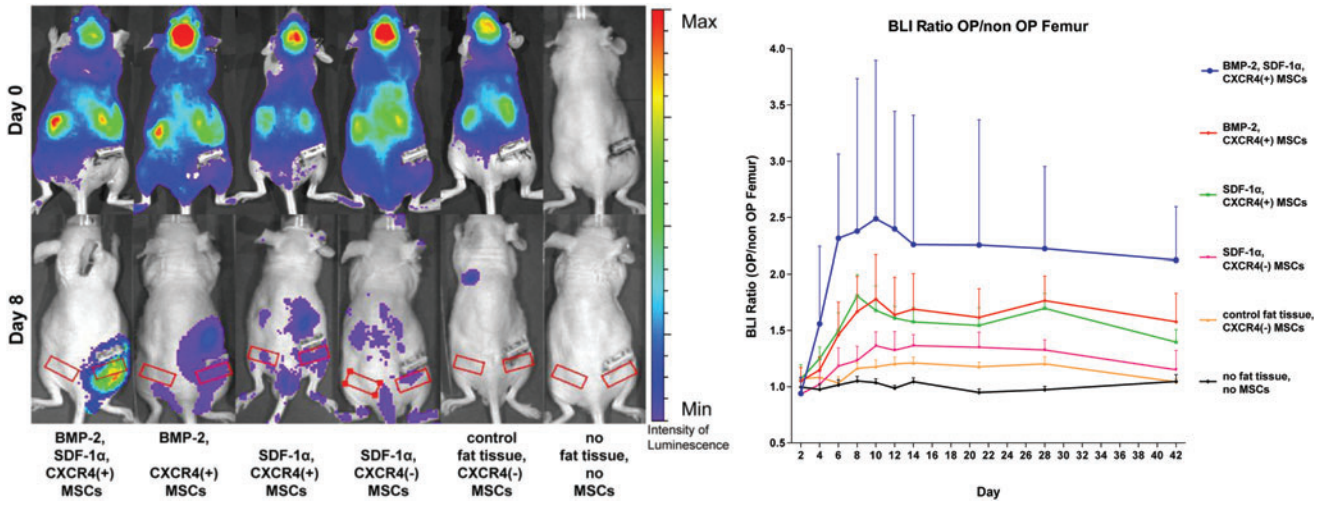

FIG. 2. MSC migration to the defect side on the right femur in the six groups. On the left side in the upper row, mice are shown 5 min postinjection indicating systemic cell distribution of reporter cells. In the lower row, mice are shown at day 8. Red rectangles indicate the regions of interest over the right and the left femur diaphysis. The graph on the right side shows the ratio of the luminescent signal on the right (OP) versus the left femur (non-OP) (quantitative analysis). A comparison of all groups showed statistically significant differences ($p < 0.0001$, one-way ANOVA). *Post hoc* testing showed significant intergroup differences between the following treatment groups and the negative control group ($p < 0.05$, Tukey test): [BMP-2, SDF-1α, CXCR4(+) MSCs]; [BMP-2, CXCR4(+) MSCs]; [SDF-1α, CXCR4(+) MSCs]. MSC, mesenchymal stromal cell. Color images available online at www.liebertpub.com/tea

evaluate bone metabolism (Fig. 6). There was a trend to more bone formation in the BMP-2, SDF-1α, CXCR4(+) MSC group than in all other groups, since more osteoblasts were found in these sections. However, there were no significant differences as the intragroup standard deviation was comparatively high.

Discussion

Using a murine critical size segmental bone defect model, this study demonstrated that the combination of the cytokine SDF-1α and the growth factor BMP-2 had a significant positive effect on bone healing and the attraction of MSCs.

Recent studies showed that bone marrow-derived progenitor cells were attracted by BMP-2,[19] however, the exact molecular mechanisms involved in this chemoattractive effect are unknown. A potential approach to clarify this issue was given by Otsuru *et al.*[20] who demonstrated in a murine model that SDF-1α expression by vascular cells surrounding BMP-2 implants was strongly increased after 7 days, compared with collagen control implants. Around BMP-2 implants, a hypoxia inducible factor-1-dependent initial

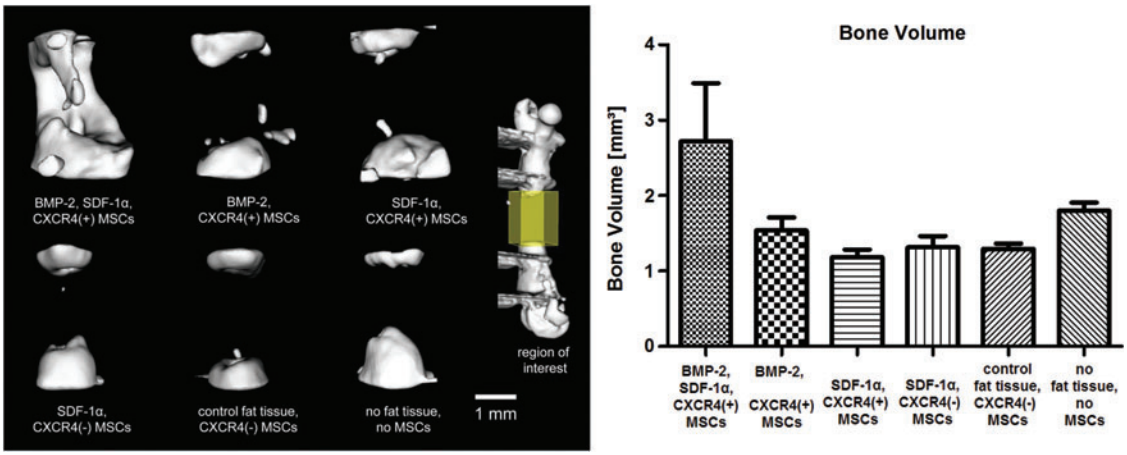

FIG. 3. Microcomputed tomography determination of bone volume at the defect side after a 6-week follow-up. On the left side, representative three-dimensional reconstructions of the defect area are shown in the different groups. The graph on the right side shows mean and 95% confidence interval resulting from the quantitative analysis of each group. Intergroup comparison showed statistically significant differences ($p < 0.0001$, one-way ANOVA). *Post hoc* testing showed significant intergroup differences between [BMP-2, SDF-1α, CXCR4(+) MSC] group and the negative control group ($p < 0.05$, Tukey test). Color images available online at www.liebertpub.com/tea

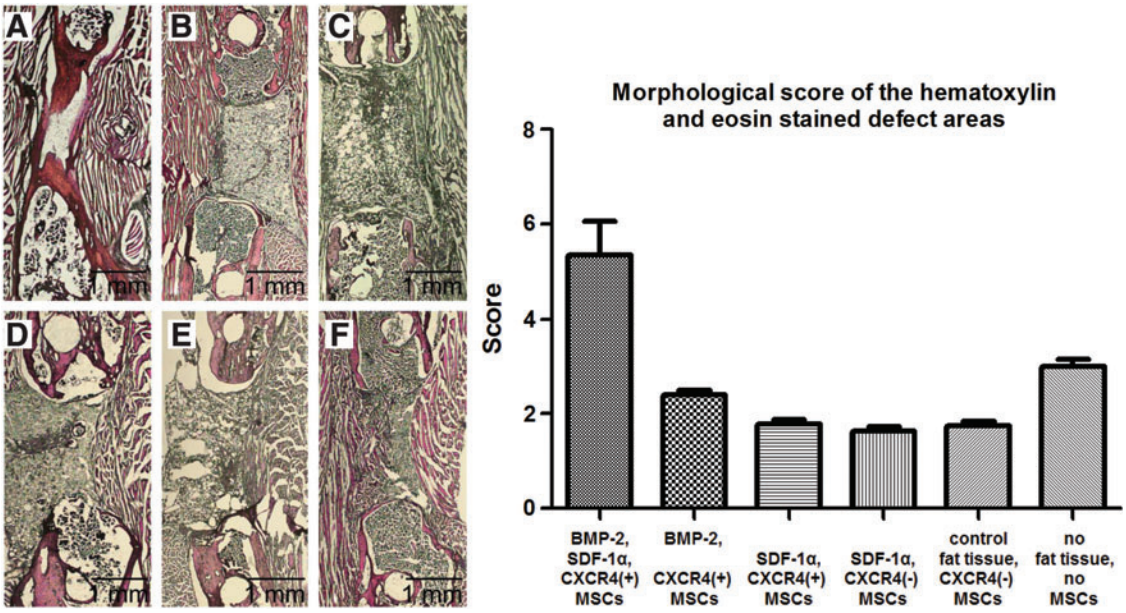

FIG. 4. Morphological scoring of the hematoxylin and eosin (H&E) stained defect areas according to Huo *et al.*[18] On the left side, representative H&E stained sections are shown for each group **[A:** BMP-2, SDF-1α, CXCR4(+) MSCs; **B:** BMP-2, CXCR4(+) MSCs; **C:** SDF-1α, CXCR4(+) MSCs; **D:** SDF-1α, CXCR4(−) MSCs; **E:** control fat tissue, CXCR4(−) MSCs; **F:** no fat tissue, no MSCs**]**. The graph on the right side shows the mean score mean and 95% confidence interval resulting from the semiquantitative analysis of each group. A comparison of all groups showed statistically significant differences ($p < 0.0001$, one-way ANOVA). *Post hoc* testing showed significant intergroup differences between the following treatment groups and the negative control group ($p < 0.05$, Tukey test): [BMP-2, SDF-1α, CXCR4(+) MSCs]; [SDF-1α, CXCR4(+) MSCs]; [SDF-1α, CXCR4(−) MSCs]; [control fat tissue, CXCR4(−) MSCs]. Color images available online at www.liebertpub.com/tea

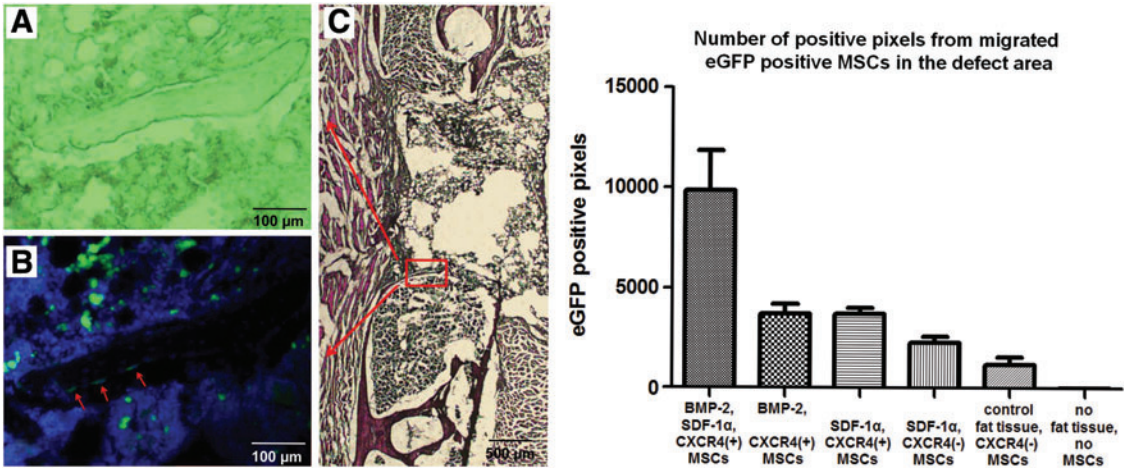

FIG. 5. Migrated MSCs in the defect area. On the left side, representative histological sections of group SDF-1α, CXCR4(+) MSCs are shown. **(A)** Shows the unstained bright view of a newly formed bone bridge surrounded by fibrous tissue, fat tissue graft (superior), and bone marrow (inferior). **(B)** Showing the same view as **(A)**, presents fluorescence imaging. Enhanced green fluorescent protein (eGFP)-labeled cells are shown in green (migrated MSCs), all 4′ 6-diamidino-2-phenylindole (DAPI) stained nuclei are shown in blue. Most of the migrated MSCs are located in the fibrous tissue and the fat tissue graft. However, some of the migrated MSCs are incorporated in the bone bridge (labeled with red arrows). **(C)** Shows the H&E overview, which indicates the location of **(A, B)**. The graph on the right side shows the number of eGFP-positive pixels (from migrated MSCs) of the whole defect area. Mean and 95% confidence interval for each group are presented (quantitative analysis). A comparison of all groups showed statistically significant differences ($p < 0.0001$, one-way ANOVA). *Post hoc* testing showed significant intergroup differences between the following treatment groups and the negative control group ($p < 0.05$, Tukey test): [BMP-2, SDF-1α, CXCR4(+) MSCs]; [BMP-2, CXCR4(+) MSCs]; [SDF-1α, CXCR4(+) MSCs]; [SDF-1α, CXCR4(−) MSCs]. Color images available online at www.liebertpub.com/tea

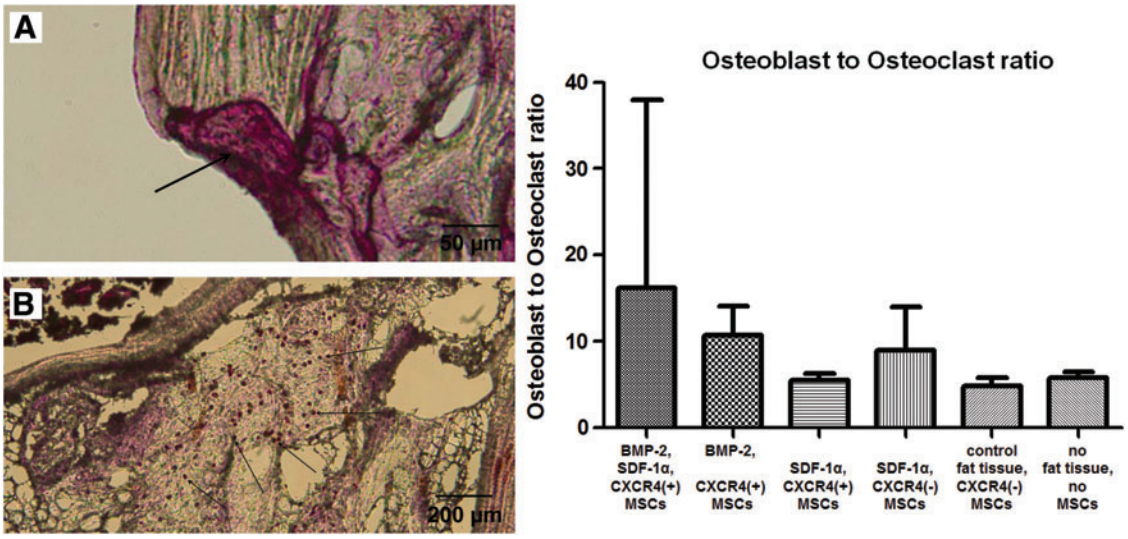

FIG. 6. Osteoblast to osteoclast ratio. On the left side, representative sections of an osteoclast **(A,** tartrate-resistant acid phosphatase stain**)** and osteoblasts are shown **(B,** alkaline phosphatase stain**)** as they were counted for the whole former defect area. The graph on the right side shows the mean osteoblast to osteoclast ratios and 95% confidence intervals for each group. A comparison of all groups showed statistically significant differences ($p < 0.0001$, one-way ANOVA). *Post hoc* testing showed no significant intergroup differences. Color images available online at www.liebertpub.com/tea

expression of SDF-1α was found in arterioles, followed by BMP-2-dependent recruitment and differentiation of the trapped bone marrow-derived progenitor cells to osteoblasts, which expressed SDF-1α.[20]

The SDF-1α/CXCR4 chemokine/ligand axis is known to be involved in the process of MSC attraction, with SDF-1α specifically binding to the CXCR-4 receptor.[21] In this context, cooperative mechanisms between several molecular pathways involving adhesion molecules, cytokines, chemokines, proteolytic enzymes, and growth factors were reported.[21] These findings can explain the effects of both BMP-2 and SDF-1α on site-specific MSC attraction observed in the present study. Additionally, we demonstrated a cumulative attraction potential when BMP-2 and SDF-1α are applied in combination.

It has been widely demonstrated *in vitro*,[22] in preclinical *in vivo* models,[23] and in clinical use[24,25] that BMP-2 is a potent osteoinductive growth factor. We observed that SDF-1α alone does not support bone regeneration. Recent findings of Higashino *et al.* partly explain why the combination of BMP-2 and SDF-1 potentiates bone formation.[13] SDF-1α recruits osteoprogenitor cells to the site of injury, thereby potentially stimulating bone formation. During fracture repair, SDF-1α is mainly released by the periosteum.[26] Upon antibody-mediated blocking of the SDF-1α/CXCR4 pathway, the effect of BMP-2 on bone formation is reduced.[13] Furthermore, Chim *et al.* found improved vascularization for the combination of both cytokines compared to applying only BMP-2 or SDF-1α alone.[27]

Both paracrine and autocrine mechanisms resulting in the secretion of cytokines and in cellular differentiation, respectively, can explain the stimulatory effect of the migrated MSCs on fracture healing. Against our expectation, the fat tissue grafts did not transform to bone tissue as was reported by others using BMP-2 activated fat tissue grafts.[15,17] According to our ELISA-based *in vitro* data, which may not most suitably represent the actual transgene release kinetics *in vivo*, it may at best be speculated that the adenovirally transduced fat tissue grafts lose their potential to express biologically active SDF-1α and BMP-2 after 2–3 weeks. The role of fat tissue as an implant for bone healing is controversial. On the one hand, it was reported that BMP-2 activated fat tissue grafts led to bone formation.[17,28] On the other hand, free fat transplants are frequently used to prevent osseous union in animals models[29] and clinically.[30–33] In this study, we found that the fat tissue inserted at the defect site prevented bone healing. If bone growth appeared, it was mainly around the fat tissue. It may be speculated that the duration of BMP-2 expression was too short and that the local concentration of this growth factor was too low. However, the design of the present study did not directly address this issue, and further research is needed to resolve this point.

Adenoviral gene therapy, primarily developed to treat genetic disorders, is currently of great interest for cancer therapy and already in clinical use.[34] It offers the ability to efficiently transduce a variety of both quiescent and proliferating cell types.[35] Adenoviral vectors can be easily grown to a very high titer, allowing for transduction of a large number of cells and/or a tissue target in large animals and humans.[35] An important safety feature includes the absence of vector genome integration, thereby reducing the likelihood for germ-line transmission and insertional mutagenesis.[35] As experience in the use of adenoviral gene therapy continues to increase, this method has potential applications for use in clinical regenerative medicine. In addition, lentiviral stem cell therapy is of potential interest for clinical applications. Whereas the first clinical trials are currently being analyzed, extended clinical validation is required to establish long-term safety of these methods.[36]

In the present study, SDF-1α or BMP-2 alone, expressed by adenoviral activated fat tissue grafts, showed negative effects on bone healing, compared with the negative control. This may indicate that the BMP-2 concentration used at the defect

site was suboptimal. In line with previous studies,[13] we were also able to confirm that in a critical size segmental bone defect, the osteoinductive potential of a low concentration of BMP-2 can be significantly enhanced in the presence of SDF-1α. In a practical translational sense, these findings suggest that the adverse effects of high doses of BMP-2 could potentially be avoided by applying low doses of BMP-2 in combination with SDF-1α.

Conclusion

Our study showed that SDF-1α enhanced bone healing induced by BMP-2. Both proteins also had a cumulative effect on reporter MSC attraction to the bone defect site.

Acknowledgments

This work was supported by the AO Foundation (Start up Grant S-10-67), the German Academic Exchange Service/ Federal Ministry of Education and Research (grant # D/09/ 04774), and by the Ellenburg Chair in Surgery, Stanford University. Bioluminescence imaging and CT scans were performed in the Stanford Small Animal Imaging Facility. We thank Prof. Alexander Harris for statistical consulting.

Disclosure Statement

No competing financial interests exist.

References

1. HCUP Databases. Healthcare Cost and Utilization Project (HCUP). Agency for Healthcare Research and Quality, Rockville, MD, 2006–2009.
2. Logeart-Avramoglou, D., Anagnostou, F., Bizios, R., and Petite, H. Engineering bone: challenges and obstacles. J Cell Mol Med **9,** 72, 2005.
3. Colterjohn, N.R., and Bednar, D.A. Procurement of bone graft from the iliac crest. An operative approach with decreased morbidity. J Bone Joint Surg Am **79,** 756, 1997.
4. Arrington, E.D., Smith, W.J., Chambers, H.G., Bucknell, A.L., and Davino, N.A. Complications of iliac crest bone graft harvesting. Clin Orthop Relat Res **329,** 300, 1996.
5. Zwingenberger, S., Nich, C., Valladares, R.D., Yao, Z., Stiehler, M., and Goodman, S.B. Recommendations and considerations for the use of biologics in orthopedic surgery. BioDrugs **26,** 245, 2012.
6. van Baardewijk, L.J., van der Ende, J., Lissenberg-Thunnissen, S., Romijn, L.M., Hawinkels, L.J., Sier, C.F., *et al.* Circulating bone morphogenetic protein levels and delayed fracture healing. Int Orthop **37,** 523, 2013.
7. Zara, J.N., Siu, R.K., Zhang, X., Shen, J., Ngo, R., Lee, M., *et al.* High doses of bone morphogenetic protein 2 induce structurally abnormal bone and inflammation *in vivo*. Tissue Eng Part A **17,** 1389, 2011.
8. Lee, K.B., Taghavi, C.E., Murray, S.S., Song, K.J., Keorochana, G., and Wang, J.C. BMP induced inflammation: a comparison of rhBMP-7 and rhBMP-2. J Orthop Res **30,** 1985, 2012.
9. Epstein, N.E. Pros, cons, and costs of Infuse in spinal surgery. Surg Neurol Int **2,** 10, 2011.
10. Carragee, E.J., Hurwitz, E.L., and Weiner, B.K. A critical review of recombinant human bone morphogenetic protein-2 trials in spinal surgery: emerging safety concerns and lessons learned. Spine J **11,** 471, 2011.
11. Einhorn, T.A. The cell and molecular biology of fracture healing. Clin Orthop Relat Res **355,** 7, 1998.
12. Thieme, S., Ryser, M., Gentsch, M., Navratiel, K., Brenner, S., Stiehler, M., *et al.* Stromal cell-derived factor-1alpha-directed chemoattraction of transiently CXCR4- overexpressing bone marrow stromal cells into functionalized three-dimensional biomimetic scaffolds. Tissue Eng Part C **15,** 687, 2009.
13. Higashino, K., Viggeswarapu, M., Bargouti, M., Liu, H., Titus, L., and Boden, S.D. Stromal cell-derived factor-1 potentiates bone morphogenetic protein-2 induced bone formation. Tissue Eng Part A **17,** 523, 2011.
14. Zwingenberger, S., Niederlohmann, E., Vater, C., Rammelt, S., Matthys, R., Bernhardt, R., *et al.* Establishment of a femoral critical size bone defect model in immunodeficient mice. J Surg Res **181,** e7, 2013.
15. Zhu, H., Guo, Z.K., Jiang, X.X., Li, H., Wang, X.Y., Yao, H.Y., *et al.* A protocol for isolation and culture of mesenchymal stem cells from mouse compact bone. Nat Protoc **5,** 550, 2010.
16. Zwingenberger, S., Yao, Z., Jacobi, A., Vater, C., Valladares, R.D., Li, C., *et al.* Stem cell attraction via SDF-1α expressing fat tissue grafts. J Biomed Mater Res A **101,** 2067, 2013.
17. Betz, O.B., Betz, V.M., Abdulazim, A., Penzkofer, R., Schmitt, B., Schroder, C., *et al.* The repair of critical size bone defects using expedited, autologous BMP-2 gene activated fat implants. Tissue Eng Part A **16,** 1093, 2010.
18. Huo, M.H., Troiano, N.W., Pelker, R.R., Gundberg, C.M., and Friedlaender, G.E. The influence of ibuprofen on fracture repair: biomechanical, biochemical, histologic, and histomorphometric parameters in rats. J Orthop Res **9,** 383, 1991.
19. Otsuru, S., Tamai, K., Yamazaki, T., Yoshikawa, H., and Kaneda, Y. Bone marrow- derived osteoblast progenitor cells in circulating blood contribute to ectopic bone formation in mice. Biochem Biophys Res Commun **354,** 453, 2007.
20. Otsuru, S., Tamai, K., Yamazaki, T., Yoshikawa, H., and Kaneda, Y. Circulating bone marrow-derived osteoblast progenitor cells are recruited to the bone-forming site by the CXCR4/stromal cell-derived factor-1 pathway. Stem Cells **26,** 223, 2008.
21. Sharma, M., Afrin, F., Satija, N., Tripathi, R.P., and Gangenahalli, G.U. Stromal-derived factor-1/CXCR4 signaling: indispensable role in homing and engraftment of hematopoietic stem cells in bone marrow. Stem Cells Dev **20,** 933, 2011.
22. Ryoo, H.M., Lee, M.H., and Kim, Y.J. Critical molecular switches involved in BMP-2- induced osteogenic differentiation of mesenchymal cells. Gene **366,** 51, 2006.
23. Floerkemeier, T., Witte, F., Nellesen, J., Thorey, F., Windhagen, H., and Wellmann, M. Repetitive recombinant human bone morphogenetic protein 2 injections improve the callus microarchitecture and mechanical stiffness in a sheep model of distraction osteogenesis. Orthop Rev **4,** e13, 2012.
24. Even, J., Eskander, M., and Kang, J. Bone morphogenetic protein in spine surgery: current and future uses. J Am Acad Orthop Surg **20,** 547, 2012.
25. Wei, S., Cai, X., Huang, J., Xu, F., Liu, X., and Wang, Q. Recombinant human BMP-2 for the treatment of open tibial fractures. Orthopedics **35,** e847, 2012.
26. Kitaori, T., Ito, H., Schwarz, E.M., Tsutsumi, R., Yoshitomi, H., Oishi, S., *et al.* Stromal cell-derived factor 1/CXCR4 signaling is critical for the recruitment of mesenchymal stem cells to the fracture site during skeletal repair in a mouse model. Arthritis Rheum **60,** 813, 2009.

27. Chim, H., Miller, E., Gliniak, C., and Alsberg, E. Stromal-cell-derived factor (SDF) 1- alpha in combination with BMP-2 and TGF-β1 induces site-directed cell homing and osteogenic and chondrogenic differentiation for tissue engineering without the requirement for cell seeding. Cell Tissue Res **350,** 89, 2012.
28. Evans, C.H., Liu, F.J., Glatt, V., Hoyland, J.A., Kirker-Head, C., Walsh, A., *et al.* Use of genetically modified muscle and fat grafts to repair defects in bone and cartilage. Eur Cell Mater **18,** 96, 2009.
29. Merikanto, J.E., Alhopuro, S., and Ritsilä, V.A. Free fat transplant prevents osseous reunion of skull defects. A new approach in the treatment of craniosynostosis. Scand J Plast Reconstr Surg Hand Surg **21,** 183, 1987.
30. Oka, K., Doi, K., Suzuki, K., Murase, T., Goto, A., Yoshikawa, H., *et al. In vivo* three-dimensional motion analysis of the forearm with radioulnar synostosis treated by the Kanaya procedure. J Orthop Res **24,** 1028, 2006.
31. Funakoshi, T., Kato, H., Minami, A., Suenaga, N., and Iwasaki, N. The use of pedicled posterior interosseous fat graft for mobilization of congenital radioulnar synostosis: a case report. J Shoulder Elbow Surg **13,** 230, 2004.
32. Kanaya, F., and Ibaraki, K. Mobilization of a congenital proximal radioulnar synostosis with use of a free vascularized fascio-fat graft. J Bone Joint Surg Am **80,** 1186, 1998.
33. Yong-Hing, K., and Tchang, S.P. Traumatic radio-ulnar synostosis treated by excision and a free fat transplant. A report of two cases. J Bone Joint Surg Br **65,** 433, 1983.
34. Kim, K.H., Dmitriev, I., O'Malley, J.P., Wang, M., Saddekni, S., You, Z., *et al.* A Phase I Clinical Trial of Ad5.SSTR/TK.RGD, a novel infectivity-enhanced bicistronic adenovirus, in patients with recurrent gynecologic cancer. Clin Cancer Res **18,** 3440, 2012.
35. Vetrini, F., and Ng, P. Gene therapy with helper-dependent adenoviral vectors: current advances and future perspectives. Viruses **2,** 1886, 2010.
36. Aiuti, A., Biasco, L., Scaramuzza, S., Ferrua, F., Cicalese, M.P., Baricordi, C., *et al.* Lentiviral hematopoietic stem cell gene therapy in patients with Wiskott-Aldrich syndrome. Science **341,** 1233151, 2013.

Address correspondence to:
Stefan Zwingenberger, MD
Department of Orthopaedics
University Hospital Carl Gustav Carus
at Technische Universität Dresden
Fetscherstraße 74
01307 Dresden
Germany

E-mail: stefan.zwingenberger@uniklinikum-dresden.de

Received: April 8, 2013
Accepted: September 25, 2013
Online Publication Date: November 12, 2013